Characteristics of Vortex Structure and Its Shear Velocity in a Scour Hole

Kim, Jin Hong

Researcher, Research institute R. D. C. 1031-7, Sa-dong, Ansan-si, Gyeonggi-do, Korea

Abstract□At downstream part of the hydraulic structures such as spillway or drainage gate, jet flow can occur by gate opening. If stream bed is not hard or bed protection is not sufficient, scour hole will be formed due to high shear stress of the jet flow. We call this primary scour. Once the scour hole is formed, a vortex occurs in it and this vortex causes additional scour. We call this secondary scour. The primary scour proceeds to downstream together with flow direction but the secondary one proceeds to upstream direction opposite to it. If the secondary one continues and reaches to the hydraulic structure, it can undermine the bottom of hydraulic structure and this will lead to failure of structure itself. Thus, it is necessary to know the physical features of the vortex structure in a scour hole, which is the main mechanism of the secondary scour. This study deals with the characteristics of the vortex structure and its shear stress which causes the secondary scour.

Keywords□Jet flow, primary scour,secondary scour, vortex structure

I. Introduction

Jet flow, which occurs by gate opening due to flood or artificial reservoir operation, can cause the primary and secondary scour. The primary scour is formed due to high shear stress of the wall jet which occurs along the stream bed and its direction proceeds to downstream. Sheet erosion occurs at the downstream part of scour hole which is characterized by the removal of a layer with a certain thickness of bottom surface. But the secondary scour is formed due to the line vortex of water and the scouring proceeds to upstream direction. The line vortex means that it has the same size and the same strength to the transverse direction. Vortex erosion occurs at the upstream part of bottom surface. hole which is characterized by the entrainment of bottom sediment due to line vortex. Fig. 1 shows the comparison between primary and secondary scour and difference between them is summarized as follows :

	Primary scour	Secondary scour
Scouring mechanism	Wall jet	Line vortex
Erosion characteristics	Sheet erosion	Vortex erosion
Scouring direction	Downstream	Upstream
Scouring guantity	Large	Small
Scouring interval	Continuous	Intermittent
Scouring intensity	Strong	Not so strong

The vortex structure, which occurs during the process of the secondary scour, must be conside-

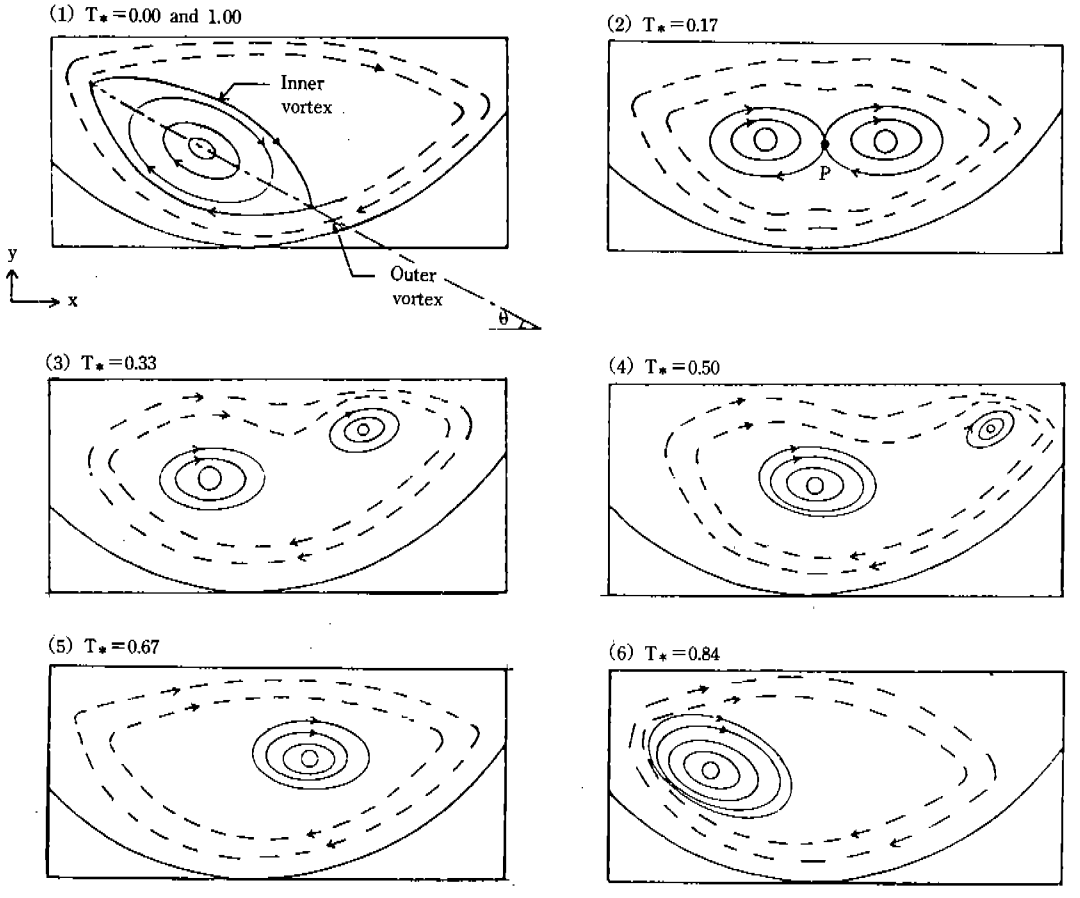

Fig. 5. Schematic diagram of the vortex motion, R1

vortex forms an inclined eye-shaped one initially as is shown in (1) of Fig. 5. Then, this vortex is divided into two horizontal eye-shaped vortices which have an equal(same magnitude and same direction) sinks shown in (2) of Fig. 5. These two vortices become apart and one of them becomes smaller finally disappeared as shown in (3), (4), and (5) of Fig. 5.

In case of a large flow(case of R6), the inclined eye-shaped vortex and a small vortex occur inside the outer large vortex. But the small vortex is unstable and sometimes disappears due to turbulence fluctuation. Its turbulence energy is very small and does not contribute to the energy dissipation in the scour hole. While, the inclined eye-shaped one has a larger but almost constant energy throughout the whole procedure. Fig. 6 shows this phenomenon. Here T_* is a dimensionless time ;

$$T_* = t/T$$

where, T is a period of one cycle of the vortex motion and t is a time corresponding to instantaneous stage of the vortex motion.

Fig. 7 shows a physical phenomenon of a vortex motion in the scour hole. An entering velocity be-

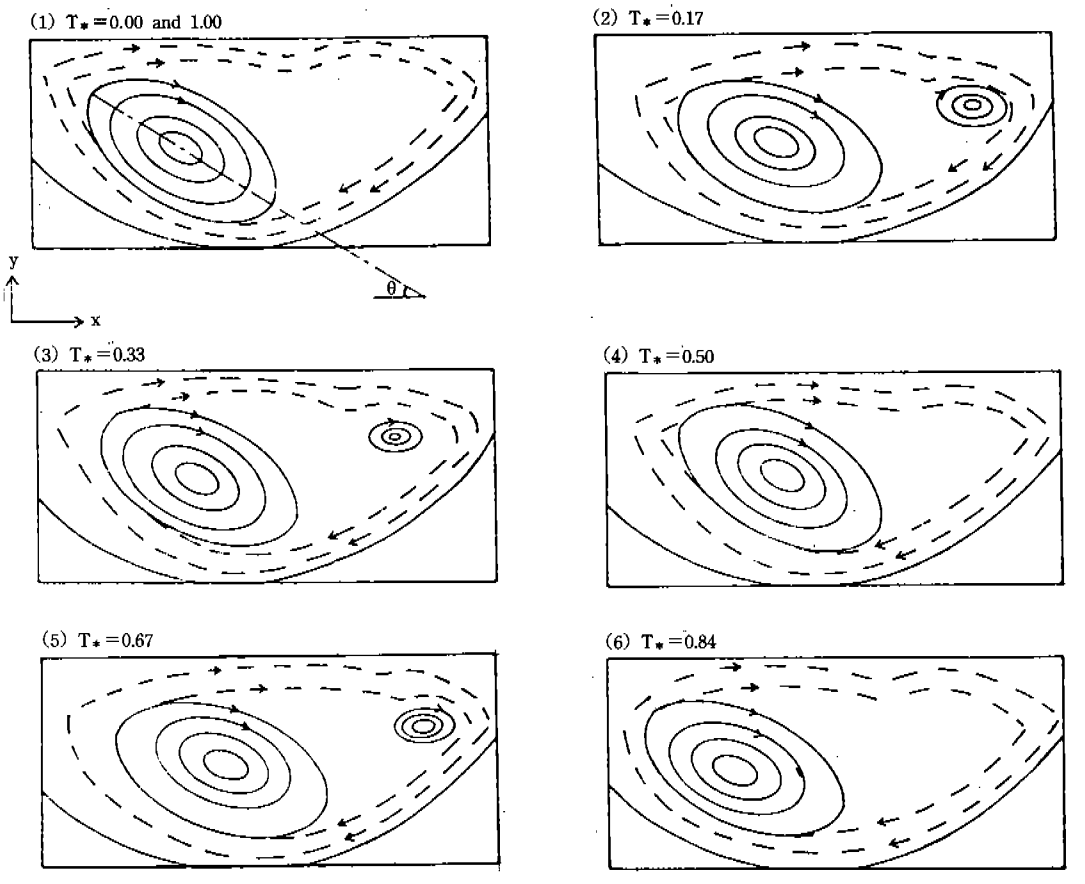

Fig. 6. Schematic diagram of the vortex motion, R6

comes accelerated from a crest to a through but becomes decelerated changing a vertical direction from the through to a crest of the downstream hump. Separation occurs at the trailing edge of a scour hole (A in Fig. 7) and reattachment occurs at the acceleration part (B in Fig. 7). These separation of the flow over a trailing edge and a subsequent reattachment lead to an outer large vortex.

Also, the inner inclined eye-shaped vortex occurs at the trailing part of the scour hole within the outer vortex. This vortex is thought to be formed due to the concentration of a vorticity which was supplied from the separation point. The axis of an inner vortex is almost parallel to the slope of downstream hump.

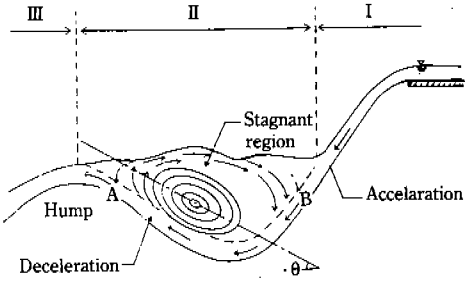

Fig. 7. Vortex motion in the scour hole

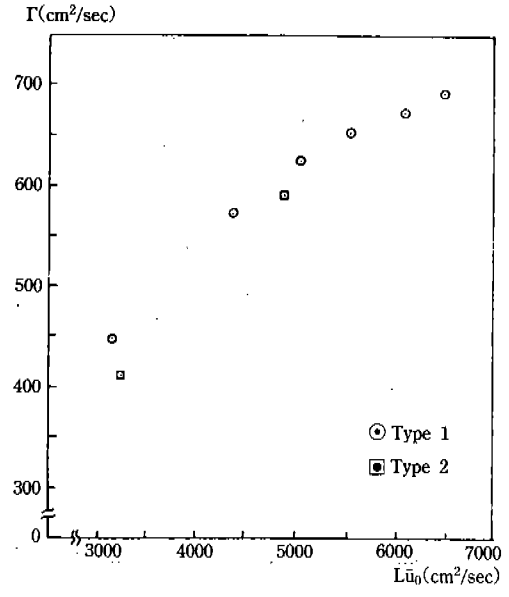

Fig. 13. Comparison between the circulation and the outer paramer

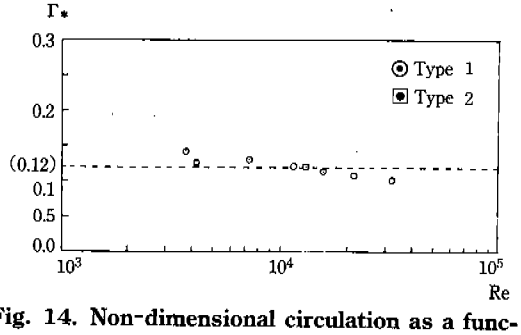

Fig. 14. Non-dimensional circulation as a function of a Reynolds number

l_x and l_y are the horizontal and the vertical scale of the vortex, respectively, and h_2 is the height of a downstream hump. As can be seen in Fig. 15, the vertical scale of the vortex is almost equal to the hump height and the horizontal scale is equal to (1.4~1.8) times of the hump height. These results are nearly the same as Tanaka (1986)'s experimental results.

While, the horizontal scale L_x and the vertical scale L_y of the outer vortex are almost equal to the length between the crests, L and the hump height, h_2, respectively, since the outer vortex consists of the separation and the reattachment of the flow and hence it occurs throughout the whole section of a scour hole.

Experimental results are summarized in Table 2, where parameters were already explained except for F_r, $\overline{W}$ and σ_s.

F_r ; upstream Froude number

$\overline{W}$; mean value of the vertical fluid velocity entrained from the trailing edge of the scour hole

σ_s ; standard deviation of the vertical turbulent velocity.

IV. Theoretical Approach and Comparison for Vortex Velocity

1. Complex Potential for the Horizontal Vortex

The eye-shaped vortices shown in (2) in Fig 5 can be analyzed theoretically as follows. The complex potential for a series of (2n+1) vortices

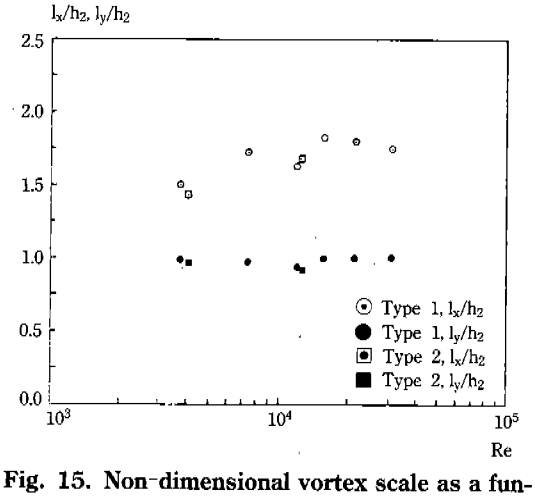

Fig. 15. Non-dimensional vortex scale as a function of Re

Table 2. Results of experiment

run no.	Re (−)	Fr (−)	lx (cm)	ly (cm)	Γ (cm²/sec)	Γ* (−)	$\bar{W}$ (cm/sec)	σ_s (cm/sec)
R1	3750	3.39	10.8	7.0	448.80	0.142	11.25	3.62
R2	7350	4.01	12.4	6.9	571.87	0.130	14.70	4.43
R3	12000	3.83	11.7	6.8	625.20	0.124	14.40	5.63
R4	15840	3.85	13.1	7.1	652.21	0.118	18.48	6.19
R5	21750	3.78	12.9	7.2	672.25	0.110	14.50	6.92
R6	30800	3.48	12.6	7.2	691.40	0.107	18.48	7.83
R7	4050	3.66	10.2	6.8	411.20	0.127	13.77	3.65
R8	12200	3.90	11.9	6.7	592.21	0.121	12.20	6.12

of the same strength Γ spaced along the x-axis at the distance a apart with the center one at the origin(Fig. 16) is.

$$W(z)=\frac{-i\Gamma}{2\pi}\ln\frac{\pi z}{a}\left(1-\frac{z^2}{a^2}\right)\left(1-\frac{z^2}{4a^2}\right)\cdots\left(1-\frac{z^2}{n^2a^2}\right)+\text{const.} \quad (3)$$

When $n\to\infty$, this may be written

$$W(z)=-\frac{i\Gamma}{2\pi}\ln\left(\sin\frac{\pi z}{a}\right)$$

$$=\frac{\Gamma}{2\pi_i}\ln\left(\sin\frac{\pi z}{a}\right) \quad (4)$$

neglecting constant terms, which have no bearing on the velocity. The velocity can be obtained from the complex potential.

$$-\frac{dW}{dz}=u-iv=+\frac{i\Gamma}{2a}\cot\frac{\pi z}{a},\quad z=x+yi$$

$$=\frac{i\Gamma}{2a}\frac{\cos\frac{\pi}{a}(x+yi)}{\sin\frac{\pi}{a}(x+yi)}$$

$$=\frac{i\Gamma}{2a}\frac{\cos\frac{\pi x}{a}\cosh\frac{\pi y}{a}-i\sin\frac{\pi x}{a}\sinh\frac{\pi y}{a}}{\sin\frac{\pi x}{a}\cosh\frac{\pi y}{a}+i\cos\frac{\pi x}{a}\sinh\frac{\pi y}{a}}$$

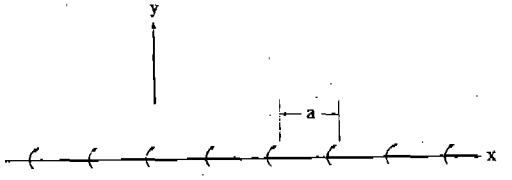

Fig. 16. Infinite row of the vortices

$$=\frac{i\Gamma}{2a}\frac{\sin\frac{2}{a}\pi x-i\sinh\frac{2}{a}\pi y}{\cosh\frac{2}{a}\pi y-\cos\frac{2}{a}\pi x} \quad (5)$$

separating into real and pure imaginary parts,

$$u=\frac{\Gamma}{2a}\frac{\sinh\frac{2}{a}\pi y}{\cosh\frac{2}{a}\pi y-\cos\frac{2}{a}\pi x}$$

$$v=\frac{-\Gamma}{2a}\frac{\sin\frac{2}{a}\pi x}{\cosh\frac{2}{a}\pi y-\cos\frac{2}{a}\pi x} \quad (6)$$

Fig. 17 shows the streamline and the equi-potential line for one of a series vortices and Fig. 18 shows the streamline for two vortices of a series vortices. Saddle point P appears at the center and with this the velocities become counter-balanced.

Fig. 18 corresponds to the theoretical streamline

$$\psi = \frac{\partial v}{\partial x} - \frac{\partial u}{\partial y} \qquad (11)$$
$$= 0$$

Flow becomes irrotational but the circulation around the origin (0, 0) is not zero. This is because the highly concentrated vorticity, i.e., vortex filament, exists at the origin.

3) In (2) of Fig. 21, point (± 0.5, 0) are saddle and the vertical velocity becomes zero.

Comparisons of the velocities between the calculational and the experimental results are shown in Fig. 22 and Fig. 23. Here θ=0 corresponds to the horizontal inner vortex and θ=21.8 corresponds to the inclined inner vortex whose angle is supposed to be equal to the slope of the hump.

As is shown in (1), (2) of Fig. 22 and (1), (2) of Fig. 23, theoretical value of u and v become infinite at the origin with the effect of the vortex filament. But the experimental value approaches zero towards the origin supporting the concept

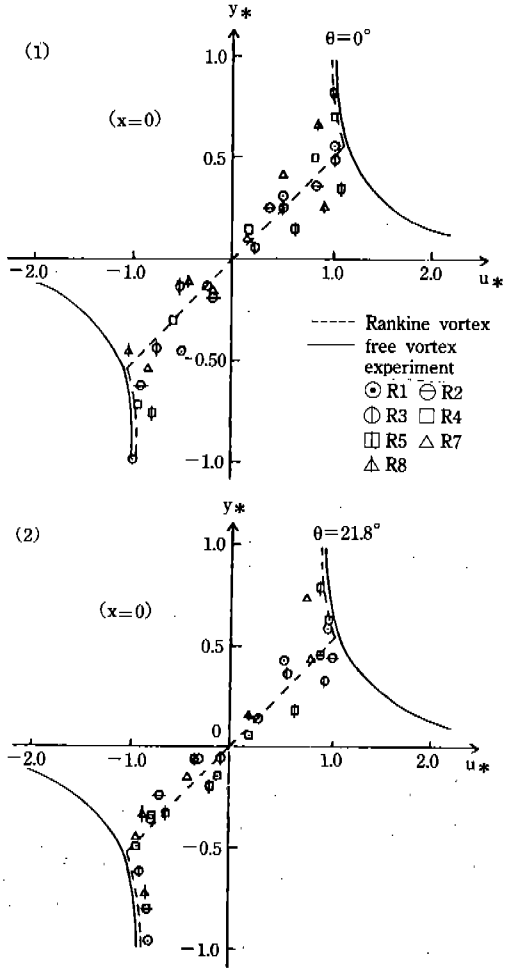

Fig. 22. Comparison of u_* between the calculation and the experimental results

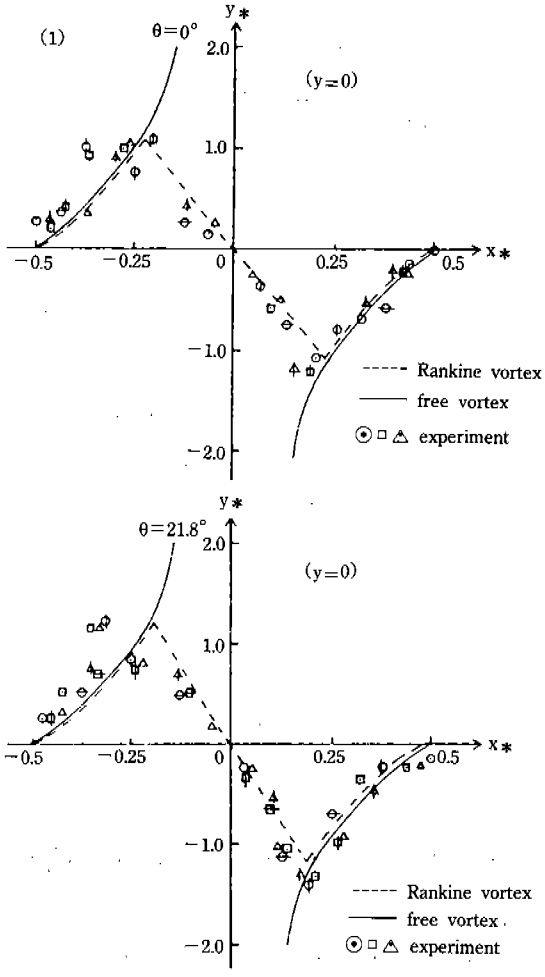

Fig. 23. Comparison of v_* between the calculation and the experimental results

of a Rankine's combined vortex, velocity profile of which is represented by the following equations.

$$v' = \frac{x}{x_0} v, \quad -x_0 \leq x \leq x_0 \qquad (12)$$

$$v, \quad x > x_0,\ x < -x_0$$

$$u' = \frac{y}{y_0} u, \quad -y_0 \leq y \leq y_0 \qquad (13)$$

$$u, \quad y > y_0,\ y < -y_0$$

The values of x_0 and y_0 are found to be approximately 0.25a and 0.50a, respectively through the experimental results.

V. Average shear velocity in a scour hole

1. Energy conservation method

To obtain the amount of a vortex erosion in a scour hole, it is necessary to determine shear velocity of a line vortex in the scour hole corresponding to friction. The shear velocity can be obtained using the energy conservation method between two crests as is shown in Fig. 24.

where, H is a storage height, H_1 is the height of an apron,

H_2 is a height of a hump crest,

$\bar{u}_0$ is an upstream average velocity of flow.

u is the velocity of a line vortex in a scour hole,

u_{max} is the maximum velocity of a line vortex and L is the length between crests.

Difference between the rates of energy influx into and energy efflux out of the considered area is equal to the change of the kinetic energy of the vortex generated in a scour hole, energy loss

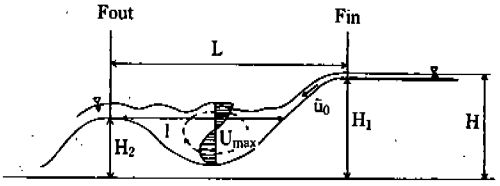

Fig. 24. Definition sketch for energy conservation method

per unit time due to skin friction along the bed of a scour hole and the energy loss per unit time due to turbulent fluctuation in a scour hole. Thus,

$$Fin-Fout = \partial(E_v+E_t)/\partial t - E_1/time \qquad (14)$$

where, Fin is an energy influx coming into a section1

$$= qgH_0, \qquad (15)$$

Fout is an energy efflux going out of a section 2 which consists of potential energy and kinetic energy

$$= qg(H_2+v_2^2/2g). \qquad (16)$$

$\partial E_v/\partial t$ is change of a kinetic energy of the vortex generated in a scour hole

$$= \frac{\partial}{\partial t}\left(\frac{1}{V/Q}\int \frac{u^2}{2} dA\right), \qquad (17)$$

E_1 energy loss due to friction along the bed of a scour hole

$$= -\frac{\tau}{q} L u_{max}, \qquad (18)$$

E_t is turbulence fluctuation energy in a scour hole,

q is fluid discharge per unit width,

Q is fluid discharge,

V is volume of a line vortex,

A is area occupied by a line vortex.

As can be seen in Figs. 5 and 6, the outer and inner vortices occur in a scour hole but the turbulence between them is small, or does not occur in case of the small discharge(case of R1). So, the energy dissipation in the scour hole is done mainly through these vortices (not turbulence) and hence the turbulence fluctuation energy, E_t can be neglected. Thus,

$$\text{Fin-Fout} = \partial E_v/\partial t - E_1/\text{time}$$

$$qgH_0 - qg\left(H_2 + \frac{V_2^2}{2g}\right) = \frac{\partial}{\partial t}\left(\frac{1}{V/Q}\int\frac{u^2}{2}\,dA\right) + \frac{\tau}{q}Lu_{max}$$

$$\therefore \frac{\tau}{q}(=u_*^2) = \frac{qg(H-H_2-\frac{V_2^2}{2g}) - \frac{\partial}{\partial t}\left(\frac{Q}{V}\int\frac{u^2}{2}\,dA\right)}{Lu_{max}}$$

$$= \frac{qg(H-H_2-\frac{V_2^2}{2g}) - \frac{\partial}{\partial t}\left(q\int\frac{u^2}{2}\frac{dA}{A}\right)}{Lu_{max}} \quad (19)$$

Experimential values for the above parameters and the average shear velocity, u_* by eq. (19) are shown in Table 3.

2. Extimation of mean shear velocity using outer parmaeter

According to Ikeda and Asaeda(1983), there is a linear relationship between the mean value of a vertical component of turbulent velocity, $\overline{W}$ and the longitudinal average velocity, U as described by,

$$\overline{W} = \beta' U \quad (20)$$

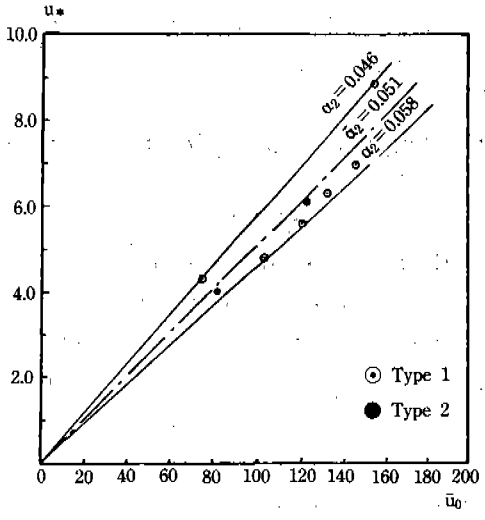

Fig. 25. Relation between $\bar{u}_0$ and u_*

Table 3. Summary of hydraulic conditions

run no.	h_0 (cm)	$\bar{u}_0$ (cm/sec)	H (cm)	H_2 (cm)	V_2 (cm/sec)	u_{max} (cm/sec)	L (cm)	u_x (cm/sec)
R1	0.5	75	10.4	7.2	70.5	25.2	41.14	4.35
R2	0.7	105	10.6	7.2	73.5	31.5	41.14	4.83
R3	1.0	120	11.1	7.2	80.0	33.1	41.14	5.65
R4	1.2	132	11.4	7.2	83.4	32.6	41.14	6.36
R5	1.5	145	11.8	7.2	87.0	35.2	41.14	7.01
R6	2.0	154	12.2	7.2	90.6	37.3	41.14	8.91
R7	0.5	81	11.5	7.2	84.3	31.2	37.20	4.05
R8	1.0	122	12.0	7.2	90.3	34.3	37.20	6.15

where, β' is a proportionality coefficient ($=0.23-0.46$).

Value of shear velocity was found to be of the same magnitude as the vertical velocity fluctuation near the trailing ridge of a sand ripple. And so,

$$\frac{u_*^2}{U^2} = \frac{W'^2}{(\bar{W}/\beta')^2} = \beta'^2 \cdot \frac{W'^2}{\bar{W}^2} = \beta'^2 \left(\frac{\overline{W-\bar{W}}^2}{\bar{W}}\right) \quad (21)$$

From the measurements over a rippled bed, Ikeda and Asaeda(1983) obtained the value of this quantity as,

$$\left(\frac{\overline{W-\bar{W}}^2}{\bar{W}}\right) \fallingdotseq 0.0324$$

Therefore, equation (21) becomes,

$$\frac{u_*^2}{U^2} = 0.0017-0.0068 \quad (22)$$

Based on the above result, the relation between the upstream mean flow velocity, $\bar{u}_0$ and the mean friction velocity, u_* in the scour hole is defined as,

$$u_* = \alpha_2 \bar{u}_0 \quad (23)$$

where, α_2 is a proportionality coefficient.

Measured values of u_* and $\bar{u}_0$ are given in Table 3 and the relations are shown in Fig. 25. Reasonable linearity is revealed between u_* and $\bar{u}_0$, where $\alpha_2=0.046-0.058$ with average value of 0.051

VI. Conclusion

Although the quantity of the secondary scour is small compared with that of the primary scour, it exerts an important effect on the stability of the hydraulic structure since the scour direction proceeds to upstream opposite to flow direction and it undermines the bottom of the hydraulic structure. In this study, characteristics of the vortex structure and its shear velocity were analyzed through experiments and compared with theoretical results. From these, circulation, vortex scale, vortex intensity and its shear velocity could be obtained with known values of inflow discharge, inflow depth and velocity. Furthermore, the amount of vortex erosion also can be obtained using the known value of the vortex intensity and the shear velocity.

References

1. Ikeda, s., and Asaeda, T. "Sediment Suspension with Rippled Bed", J. Hydr. Engrg., ASCE, 109(3), 1983.
2. Kim, J. H., Tamai, N., and Asaeda, T. "Bank Erosion due to Overflow", 44th Annual Meeting, JSCE, 1989.
3. Kim, J. H., Tamai, N., and Asaeda, T. "Unsteady Flushing of a Sand Bar by Overflow", 45th Annual Meeting, JSCE, 1990.
4. Kim, J. H. "An Experimental Study on the Vortex Structure at Downstream Part of the Hydraulic Structure", 34th Annual Meeting, KSHE, 1992.